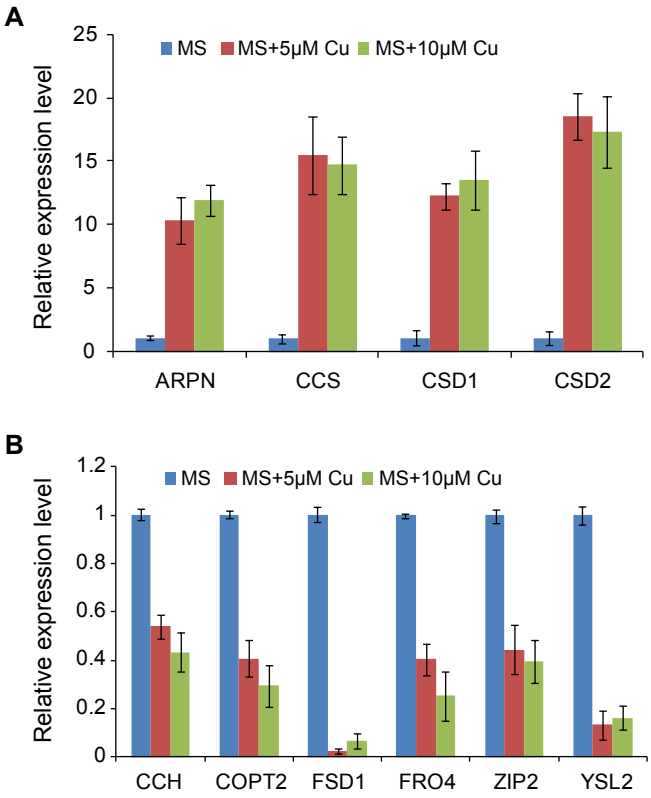

Supplemental Figure 1. Effect of Copper Regimes on the Expression of Copper-Responsive Genes in *Arabidopsis*.

(**A**) Wild-type seedlings were grown for seven days under continuous white light on agar-solidified MS media (containing 0.1 μM copper and considered insufficient), MS supplemented with 5 μM or 10 μM $CuSO_4$. Relative expression level of four representative copper-induced genes was assayed by RT-qPCR. Data shown are transcript levels relative to *ACTIN7* and set to one for the MS condition. (**B**) Relative expression levels of six copper-repressed genes under the three copper conditions. These results indicate that copper-responsive genes have comparable expression levels when either 5 or 10 μM copper supplement was used. Therefore, 5 μM was used as the copper-sufficient condition throughout this study. Data for RT-qPCR are means ± SD (n = 3).

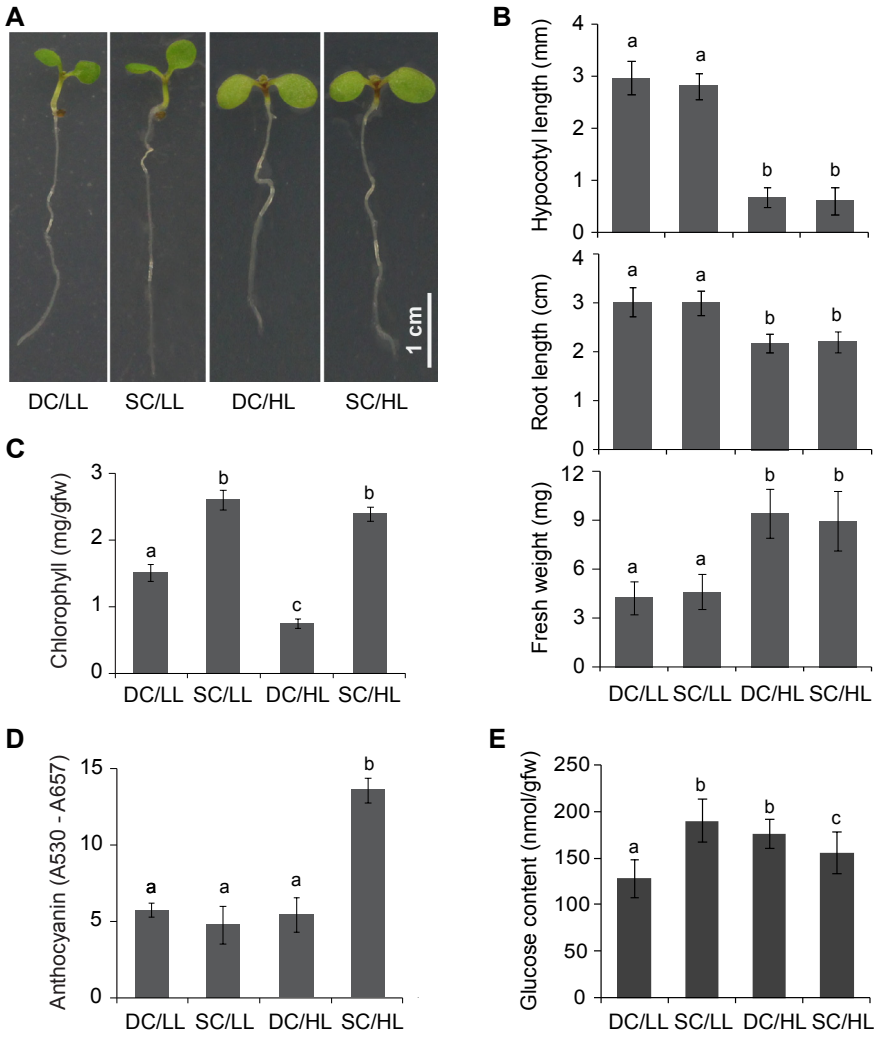

Supplemental Figure 2. Analysis of Light-copper Crosstalk in *Arabidopsis*.
(**A**) Morphology of wild type seedlings grown under the DC/LL, SC/HL, DC/LL, and SC/HL conditions. (**B**) Quantitative measurement of hypocotyl length, root length, and fresh weight of seedlings grown in the four combinations of light and copper regimes. (**C**) Total chlorophyll and (**D**) anthocyanin contents in wild type seedlings grown under the indicated conditions. Data are averages of three independent replicates. (**E**) Glucose content in the shoots of seedlings grown in four indicated conditions. Data are means ± SD (n ≥ 30 for B and n = 3 for C, D and E). Samples labeled with the same letters have no statistic difference while different letters denote groups with significant differences (ANOVA, $p < 0.01$).

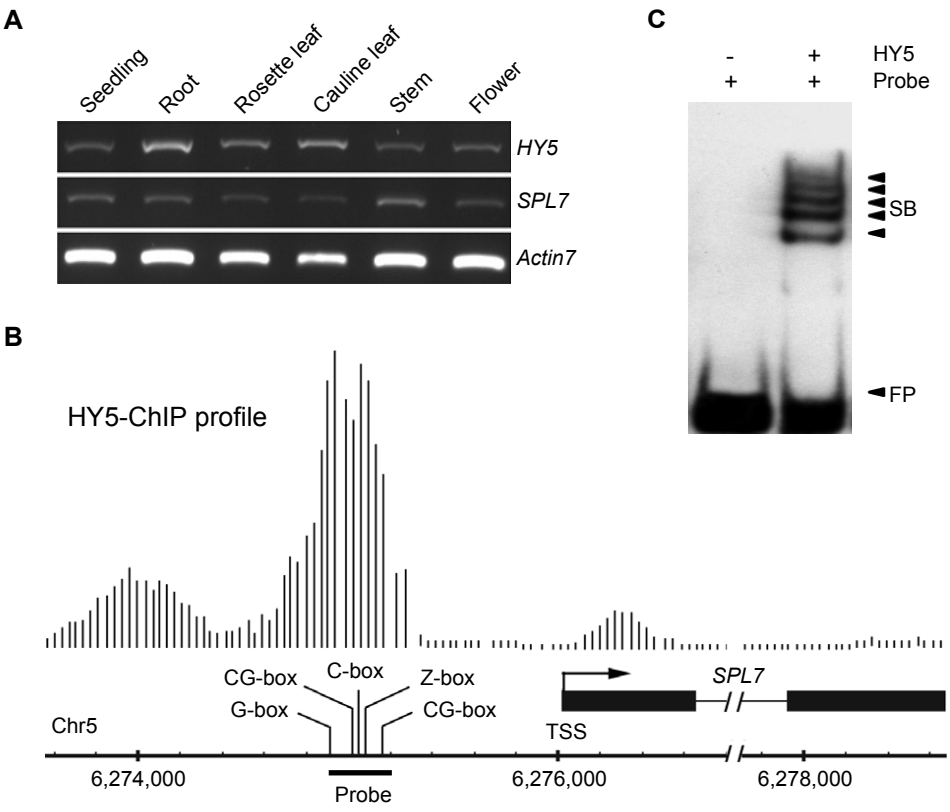

Supplemental Figure 3. HY5 directly binds to *SPL7* promoter region.
(**A**) RT-PCR analysis of the transcript levels of *HY5* and *SPL7* in young seedlings and different tissues of adult plants. *Actin7* was used as a control. (**B**) HY5 occupancy pattern at the *SPL7* locus. Raw ChIP-chip data was obtained from Zhang et al. (2011) and visualized using the Affymetrix Integrated Genome Brower. Vertical lines represent individual probes from the genome tiling microarray with height of the lines proportional to the signal intensity. Structure, transcriptional direction, and chromosomal location of *SPL7* are depicted. The G-box like motifs, TSS, and position of the probe used for EMSA are indicated as well. (**C**) EMSA analysis of HY5 binding to the *SPL7* promoter. The first lane shows only the labeled probe (-1146 to -819 from the TSS) that contains all five G-box like motifs. The second lane shows the labeled probe together with recombinant HY5 protein. Arrows indicate the free probe (FP) and the shift bands (SB).

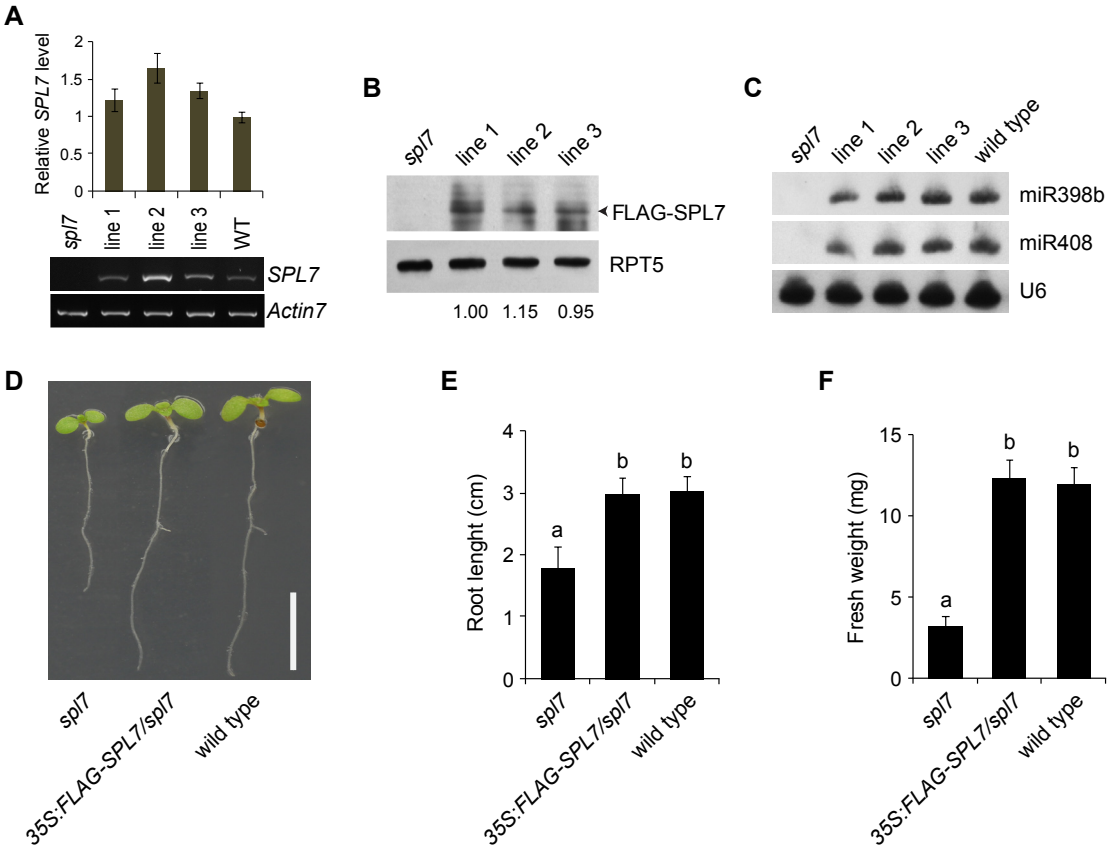

Supplemental Figure 4. Complementation of spl7 by the *35S:FLAG-SPL7* Transgene.
(**A**) FLAG-tagged SPL7 driven by the CaMV *35S* promoter was expressed in the *spl7* background (*35S:FLAG-SPL7/spl7*). Transcript levels of *SPL7* were examined in three independent lines by RT-PCR (bottom) and RT-qPCR (top) analysis. *Actin7* was used as a control. Line 1 was chosen for all subsequent experiments as it displays *SPL7* transcript level most comparable to wild type. (**B**) Immunoblot analysis of the FLAG-SPL7 protein levels in three independent transgenic lines. Total soluble protein was extracted from seedlings of each genotype grown under the low copper condition and immunoblotted with the anti-FLAG antibody. RPT5 was used as the loading control. (**C**) Expression levels of two miRNAs known to be regulated by SPL7 in the *35S:FLAG-SPL7/spl7* lines. U6 was used the loading control. (**D**) A representative transgenic plant (line 1 in A) at the seedling stage was photographed side by side with the *spl7* mutant (left) and wild type (right) seedlings grown under the low copper condition. Bar = 1 cm. (**E**) and (**F**) Quantitative measurement of fresh weight and root length of the selected *35S:FLAG-SPL7/spl7* transgenic line against wild type and *spl7* seedlings grown under the low copper condition. Data are means ± SD ($n \geq 20$). Samples labeled with the same letters have no statistic difference while different letters denote groups with significant differences (ANOVA, $p < 0.01$).

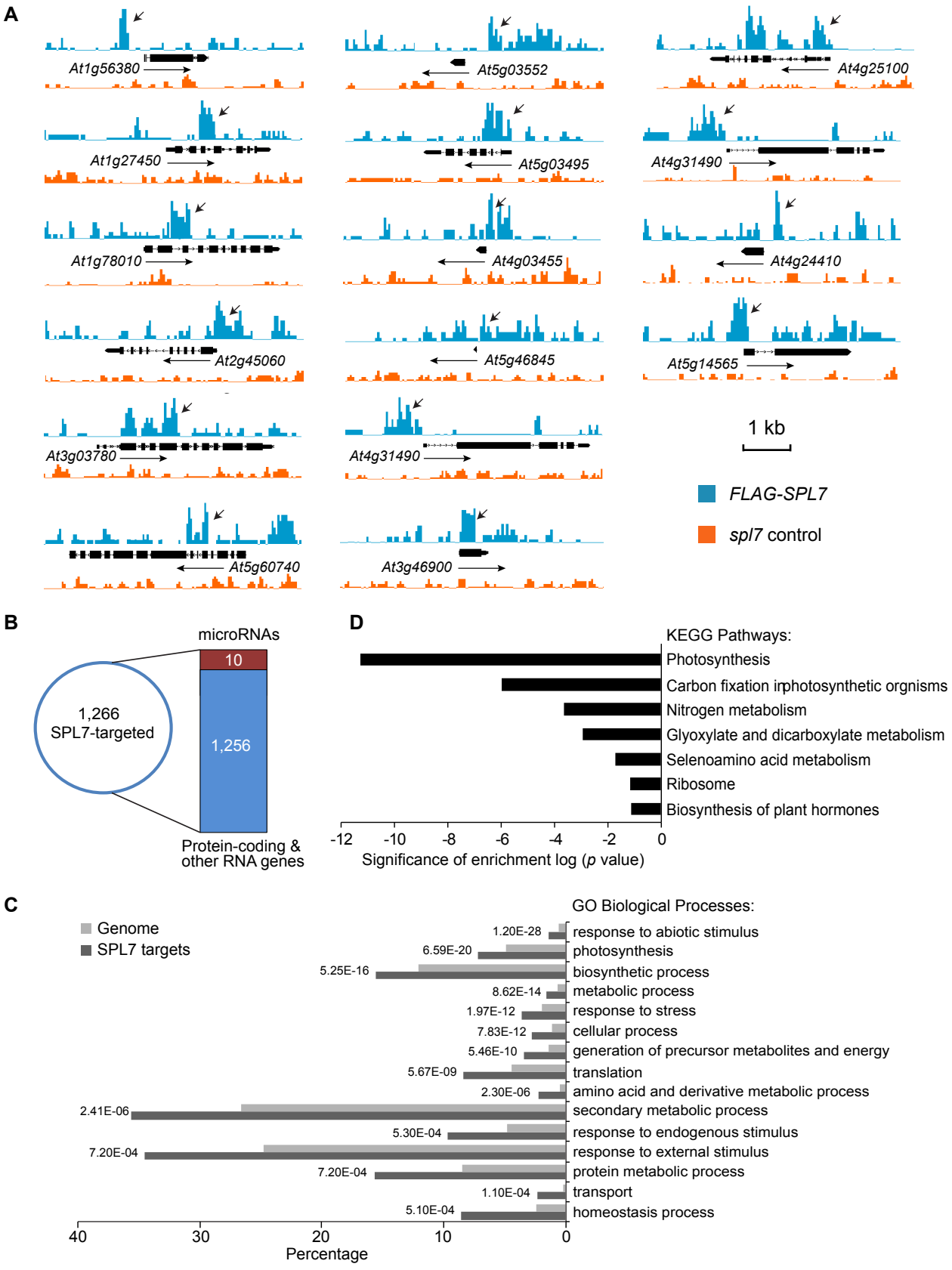

Supplemental Figure 5. Analysis of SPL7-targeted Genes.
(**A**) SPL7 binding profiles validated by ChIP-qPCR of *At1g56380*, *At5g03552(MIR822A)*, *At4g25100*, *At1g27450*, *At5g03495*, *At4g31490*, *At1g78010*, *At4g03455(MIR447B)*, *At4g24410*, *At2g45060*, *At5g46845 (MIR160C)*, *At5g14565 (MIR398C)*, *At3g03780*, *At4g31490*, *At5g60740* and *At3g46900*. ChIP-sequencing data at the selected loci were visualized using the Affymetrix Integrated Genome Brower. Vertical lines (SPL7 ChIP in blue and the negative control in orange) represent individual sequencing reads with height of the lines proportional to the copy number. Structure and transcriptional direction of the loci are depicted. Arrows indicate the binding sites selected for ChIP-qPCR validation. (**B**) SPL7 binding is associated with 1,266 genes including 10 *MIR* genes. (**C**) Enriched GO terms in the Biological Process category that are associated with the 1,266 SPL7-targeted genes. Frequencies of the GO terms for randomly selected genes from the genome and the corresponding *p* values are indicated. (**D**) Enriched pathways associated with the SPL7 targeted genes by KEGG (Kyoto encyclopedia of genes and genomes) analysis.

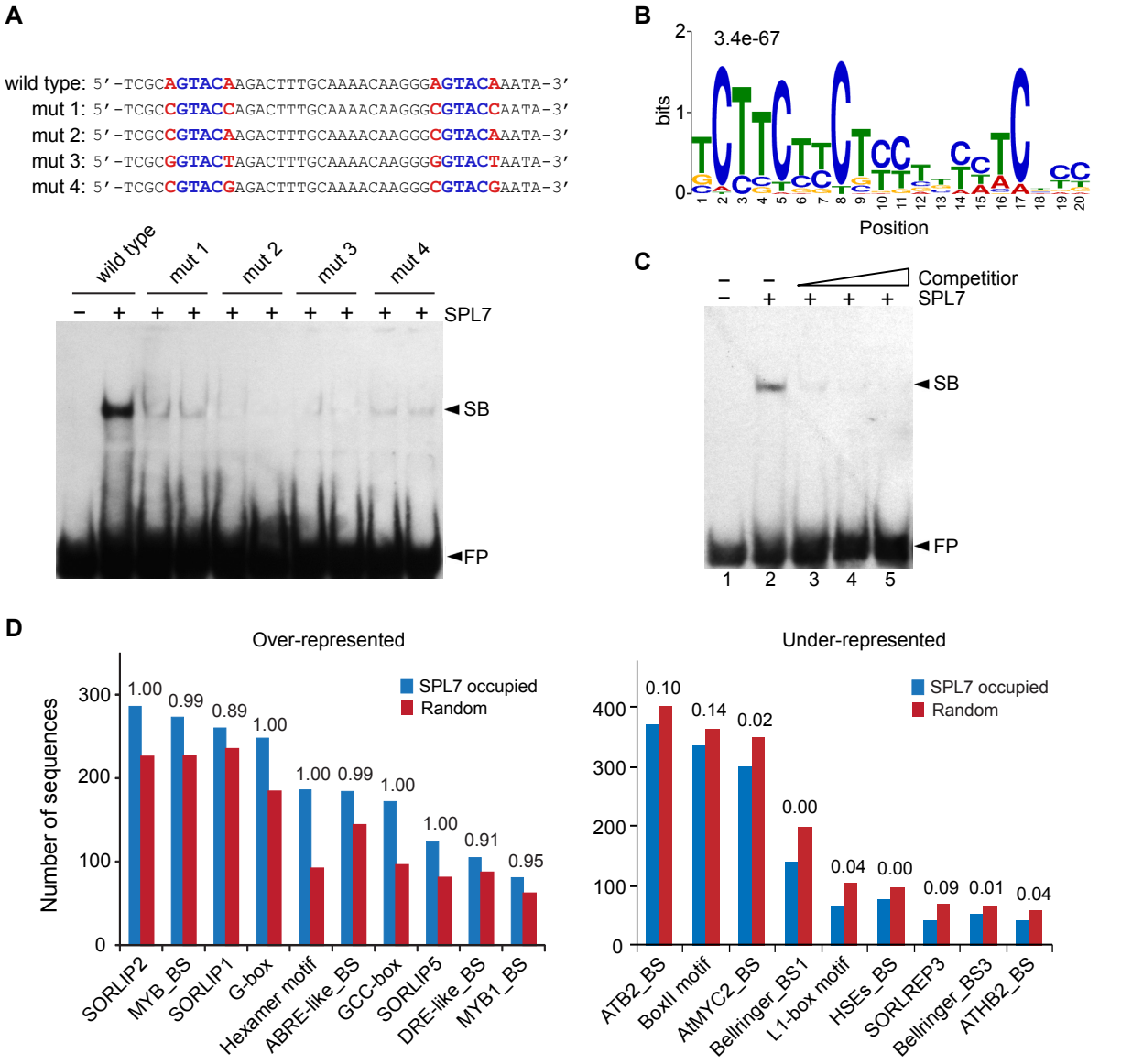

Supplemental Figure 6. Identification and Validation of Enriched DNA Elements in the SPL7 occupied Loci. (**A**) Effects of nucleotides immediately flanking the GTAC core sequence on the binding affinity for SPL7. EMSA assay was performed with recombinant SPL7 and five synthesized probes, which differ only in the two nucleotides flanking the GTAC core motif. The symmetric nucleotides (A/T) showed enhanced affinity for SPL7. (**B**) A novel consensus sequence for SPL7 binding, which was discovered in SPL7 occupied loci using the motif finder MEME. (**C**) EMSA validation of SPL7 binding to the novel motif. A probe corresponding to the consensus sequence (position from 1 to 17, TCTTCTTCTCCTTCCTC) shown in the previous panel was labeled (lane 1) and incubated with recombinant SPL7 alone (lane 2) or in the presence of unlabeled probe at different concentrations (50-fold, 100-fold, and 200-fold; lanes 3-5). (**D**) DNA elements resembling other transcription factor binding sites in SPL7-occupied regions. The SPL7 binding sites were scanned for motifs listed in the AGRIS and Transfac databases. Significantly over-represented (left) and under-represented (right) motifs are shown. Numbers represent posterior probability for P*spl7* > P*genome* which was calculated using 10,000 times Monte Carlo simulation in Matlab.

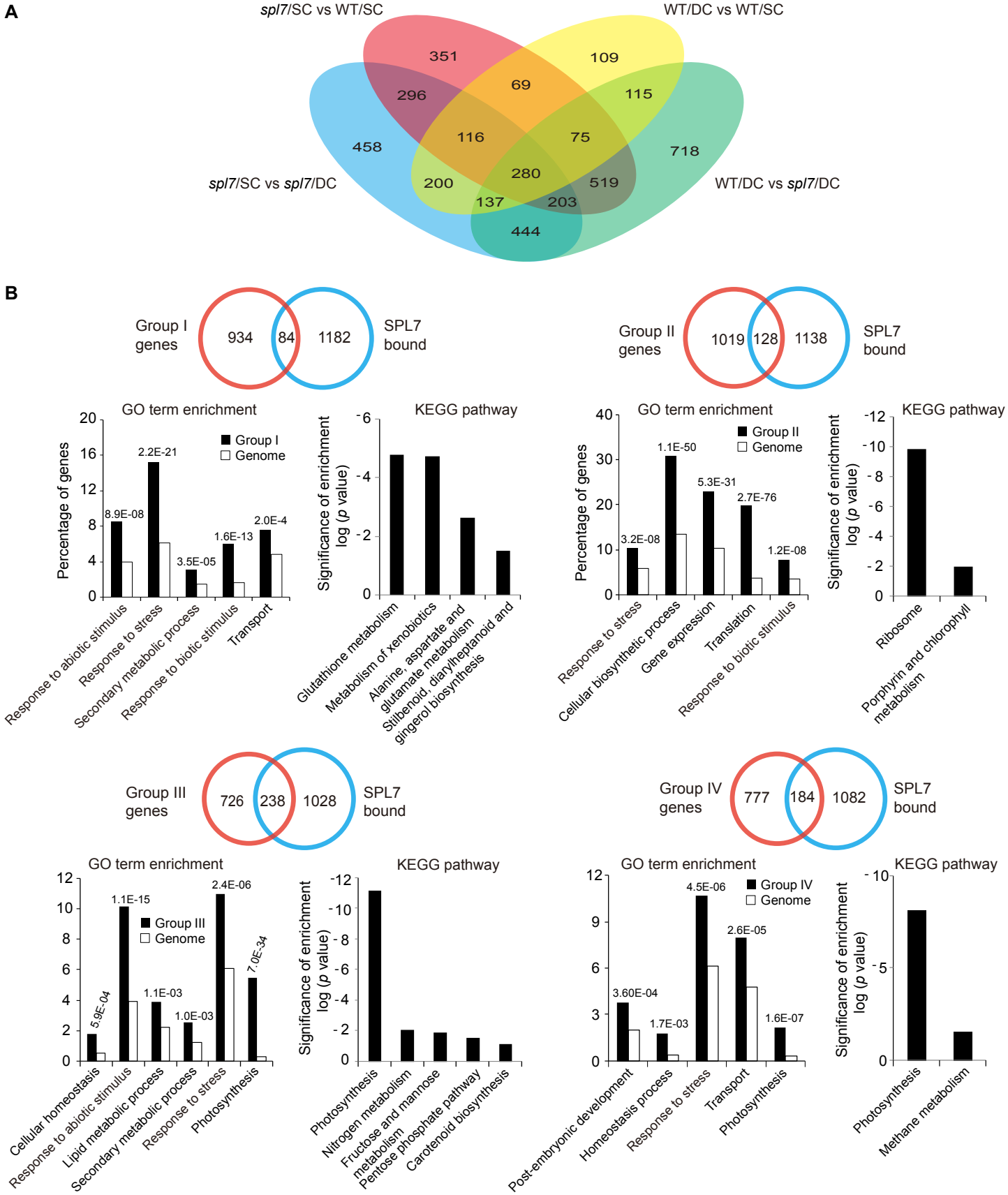

Supplemental Figure 7. Global Analysis of SPL7 Regulated Genes.
(**A**) Venn diagram depicting differentially expression genes among the four pairwise comparisons as indicated. (**B**) Detailed analysis of the four groups of genes as indicated in Figure 2 E in the main text. For each group, three panels are shown. The top panel is Venn diagram showing the overlapping between that group and SPL7 bound genes. Bottom left panel shows frequency of significantly enriched GO terms associated with genes in that group (black bar). Randomly selected genes from the genome (open bar) were used as control and the corresponding P values indicated. Bottom right panel shows KEGG pathway analysis.

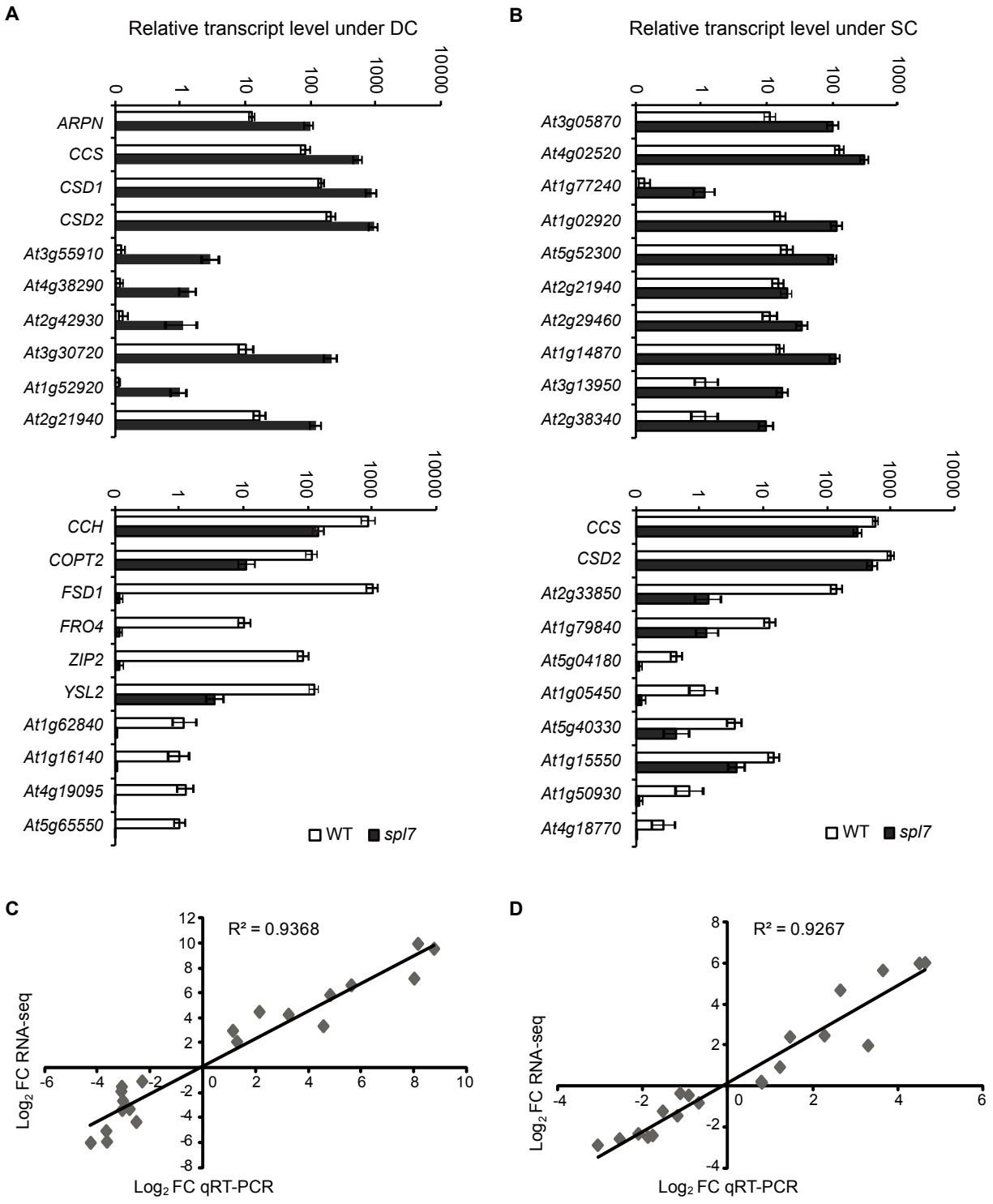

Supplemental Figure 8. Validation of RNA-sequencing Data by RT-qPCR.

(**A**) and (**B**) RT-qPCR analysis of the relative transcript levels of copper-responsive as well as randomly selected genes in WT and *spl7* seedlings grown under the DC (**A**) and SC (**B**) conditions. Data shown are transcript levels relative to *ACTIN7* as a constitutively expressed control gene, and multiplied by a factor of 1000. Values are means ± SD (n = 3). (**C**) and (**D**) Correlation between RNA-sequencing and RT-qPCR data on the selected genes under the DC (**C**) and SC (**D**) conditions. Pearson correlation was calculated using data points representing Log_2 transformed transcript level ratios between WT and the *spl7* mutant.

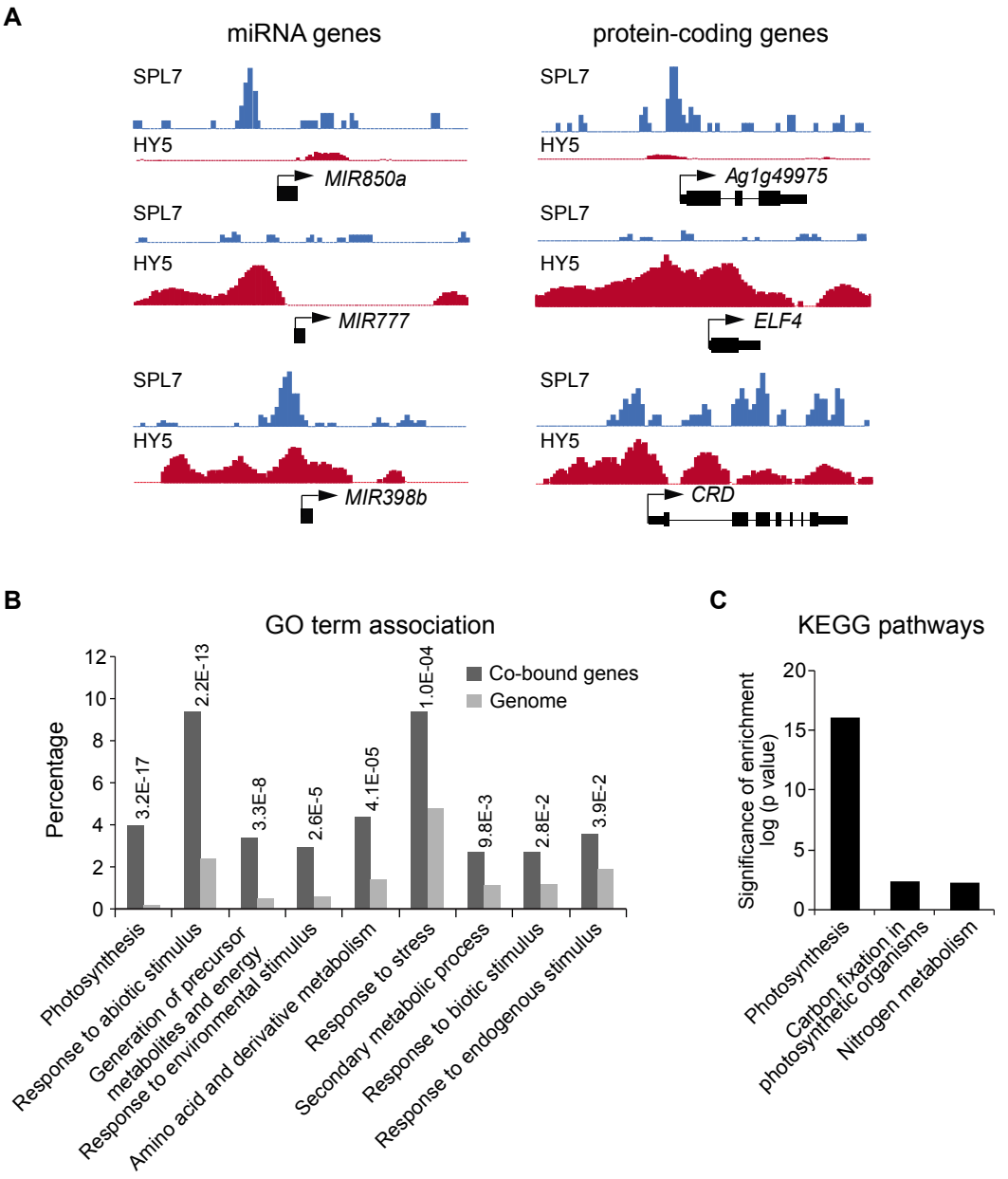

Supplemental Figure 9. Analysis of Genes Co-bound by SPL7 and HY5.
(**A**) Representative examples of the 586 genes co-bound by SPL7 and HY5 as shown in Figure 3C in the main text. For each gene, SPL7 (blue) and HY5 (red) binding patterns are visualized using the Affymetrix Integrated Genome Browser. The left and right column includes three MIR and three protein-coding genes, respectively. For each column, the gene on top is bound primarily by SPL7, the gene in the middle is primarily bound by HY5, and the gene on the bottom is co-bound by both SPL7 and HY5. (**B**) Enriched GO terms in association with the 586 genes with both SPL7 and HY5 binding. Frequencies of the GO terms for randomly selected genes from the genome and the corresponding P values are indicated. (**C**) KEGG pathway enrichment analysis of SPL7-HY5 co-bound genes.

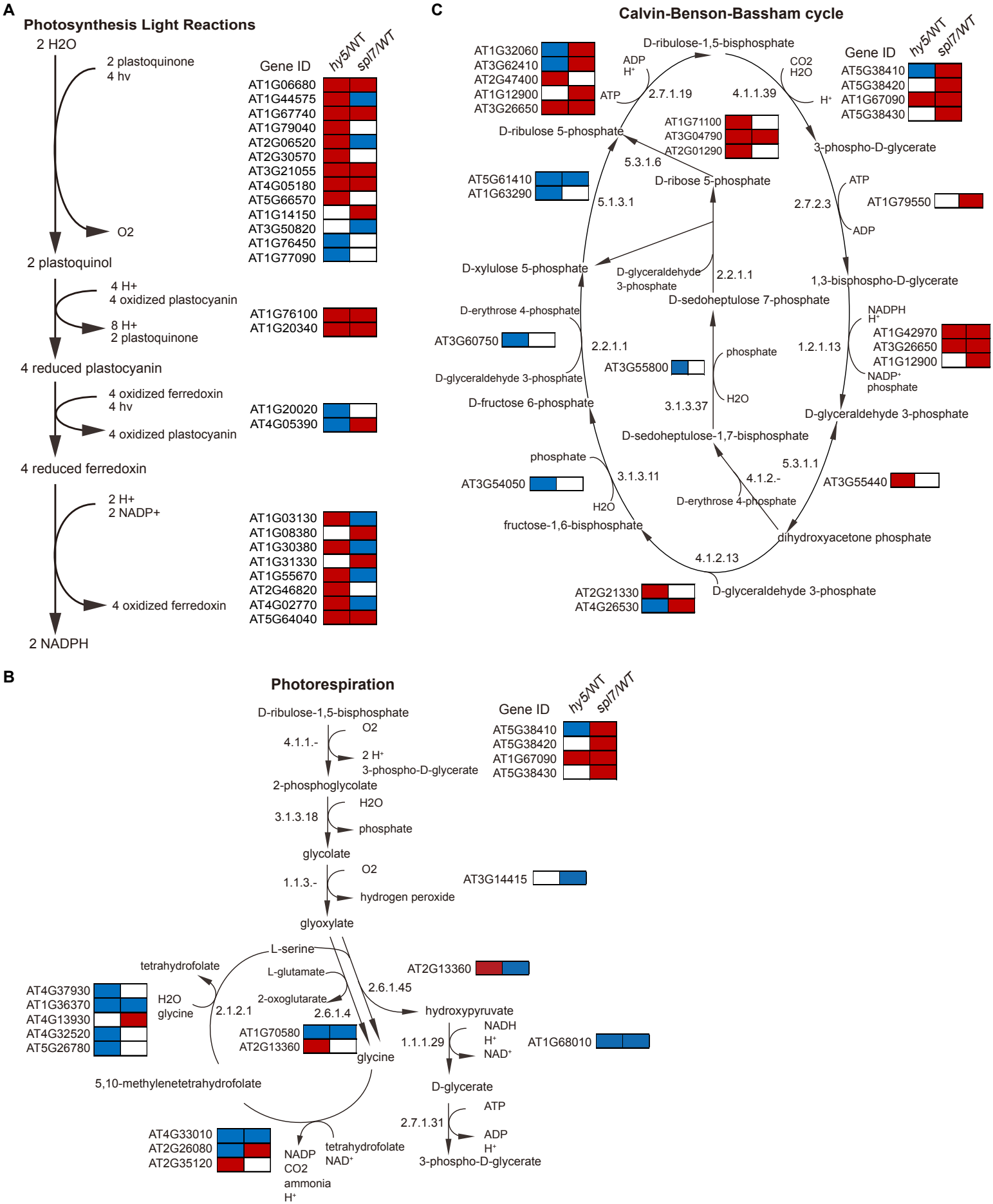

Supplemental Figure 10. *SPL7* and *HY5* Coordinatedly Regulate Photosynthesis.
(A) Genes involved in the light reactions of photosynthesis, (**B**) photorespiration, and (**C**) Calvin-Benson-Bassham cycle, are coordinately regulated by *SPL7* and *HY5*. In each panel, biochemical steps in the process as well as the corresponding enzymes are depicted. Boxes represent differentially expressed genes in either spl7 or hy5 that are involved in the pathway. Relative expression levels of these genes in either *spl7* or *hy5* are shaded with different colors with red indicating reduced expression in *spl7* or *hy5*, blue indicating increased expression in *spl7* or *hy5*, and blank indicating no significant change in *spl7* or *hy5* compared to wild type.

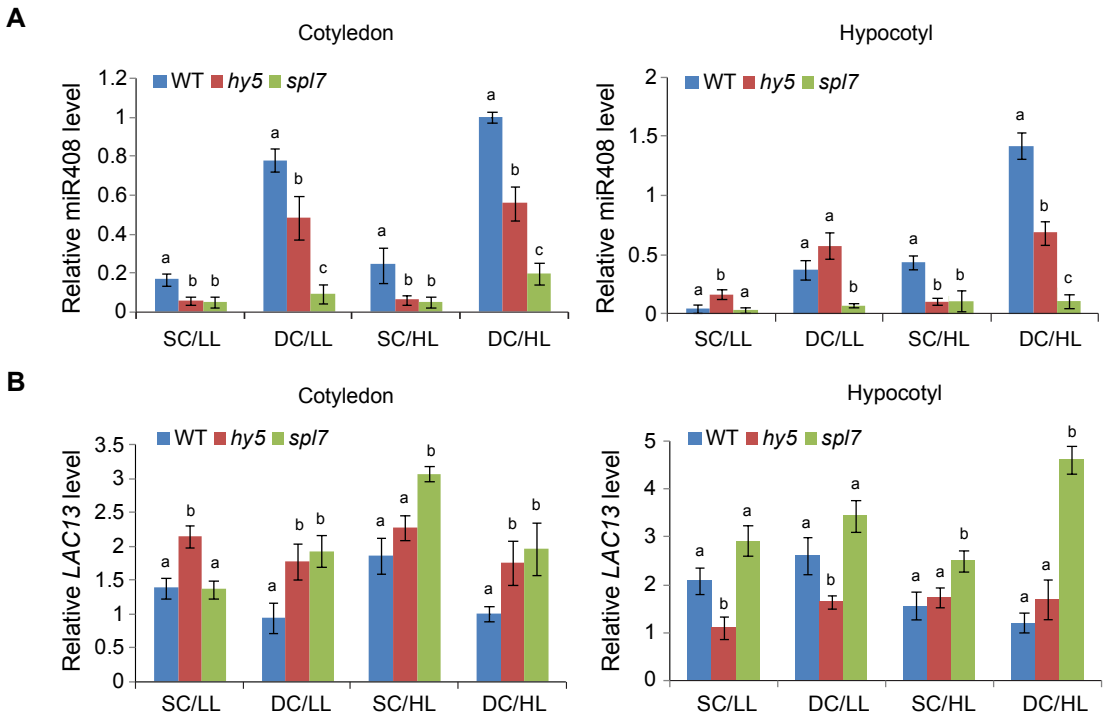

Supplemental Figure 11. Expression of *MIR408* and *LAC13* in Cotyledon and Hypocotyls.
(**A**) *MIR408* and (**B**) *LAC13* transcript levels in cotyledon and hypocotyl tissues. Total RNA was prepared separately from cotyledon and hypocotyl tissues of WT, *hy5*, and *spl7* seedlings grown under four different light and copper regimes as indicated. Following reverse transcription, relative abundance of *MIR408* and *LAC13* were determined by qPCR. For comparison, levels of *MIR408* and *LAC13* in wild type cotyledon under the DC/HL condition were set as one. Data are means ± SD (n = 3). Samples labeled with the same letters have no statistic difference while different letters denote groups with significant differences (ANOVA, $p < 0.01$).

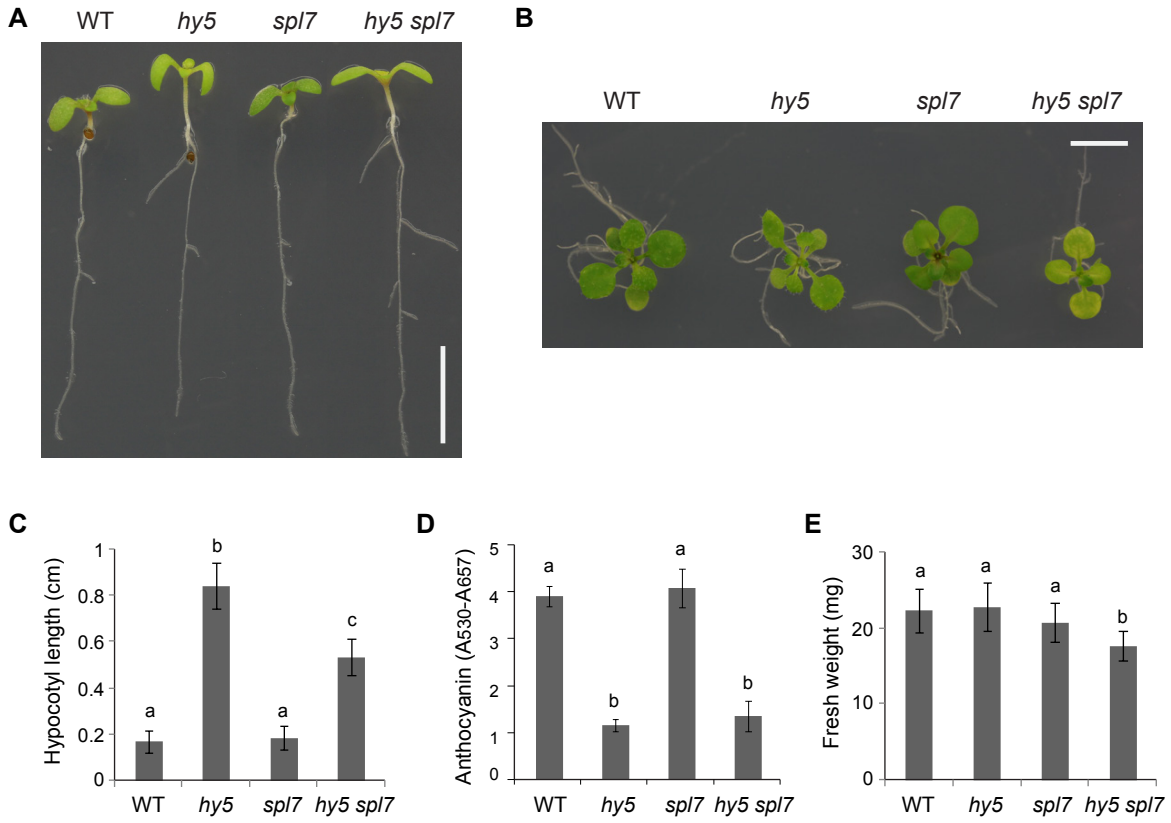

Supplemental Figure 12. Effects of Sufficient Copper on the *hy5 spl7* Double Mutant.
(**A**) Morphology of seven-day-old seedlings, and (**B**) Two-week-old adult plants grown in the SC condition. Wild type, *hy5*, *spl7*, and *hy5 spl7* plants were photographed side by side. Bars = 1cm. (**C**) Quantitative measurement of hypocotyl length of wild type, *hy5, spl7*, and *hy5 spl7* seedlings grown in SC (n ≥ 30). (**D**) Anthocyanin content in wild type, *hy5, spl7*, and *hy5 spl7* adult plants (n = 4). (**E**) Fresh weight of the four genotypes (n ≥ 50). Data are means ± SD. Genotypes labeled with the same letters have no statistical difference while different letters denote genotypes with significant differences (ANOVA, $p < 0.01$).

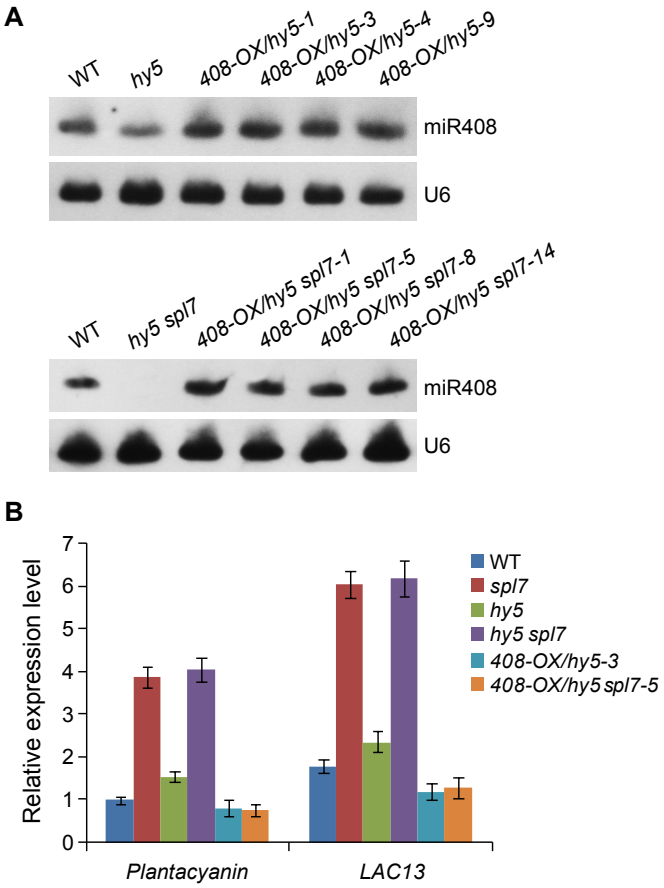

Supplemental Figure 13. Functional Analysis of *MIR408*.
(**A**) *MIR408* is constitutively activated in *hy5* (top panel) and *hy5 spl7* (bottom panel) by introducing the *35S:pre-MIR408* transgene in the corresponding genetic backgrounds. Over accumulation of miR408 in multiple independent transgenic lines is validated by RNA gel blot. U6 was as a loading control. (**B**) RT-qPCR analysis of two miR408 target genes, *Plantacyanin* and *LAC13*, in various mutants and representative transgenic lines over-expressing *MIR408* grown in the DC/HL condition. Level of *Plantacyanin* in wild type was set as one. Data are means ± SD (n=3).

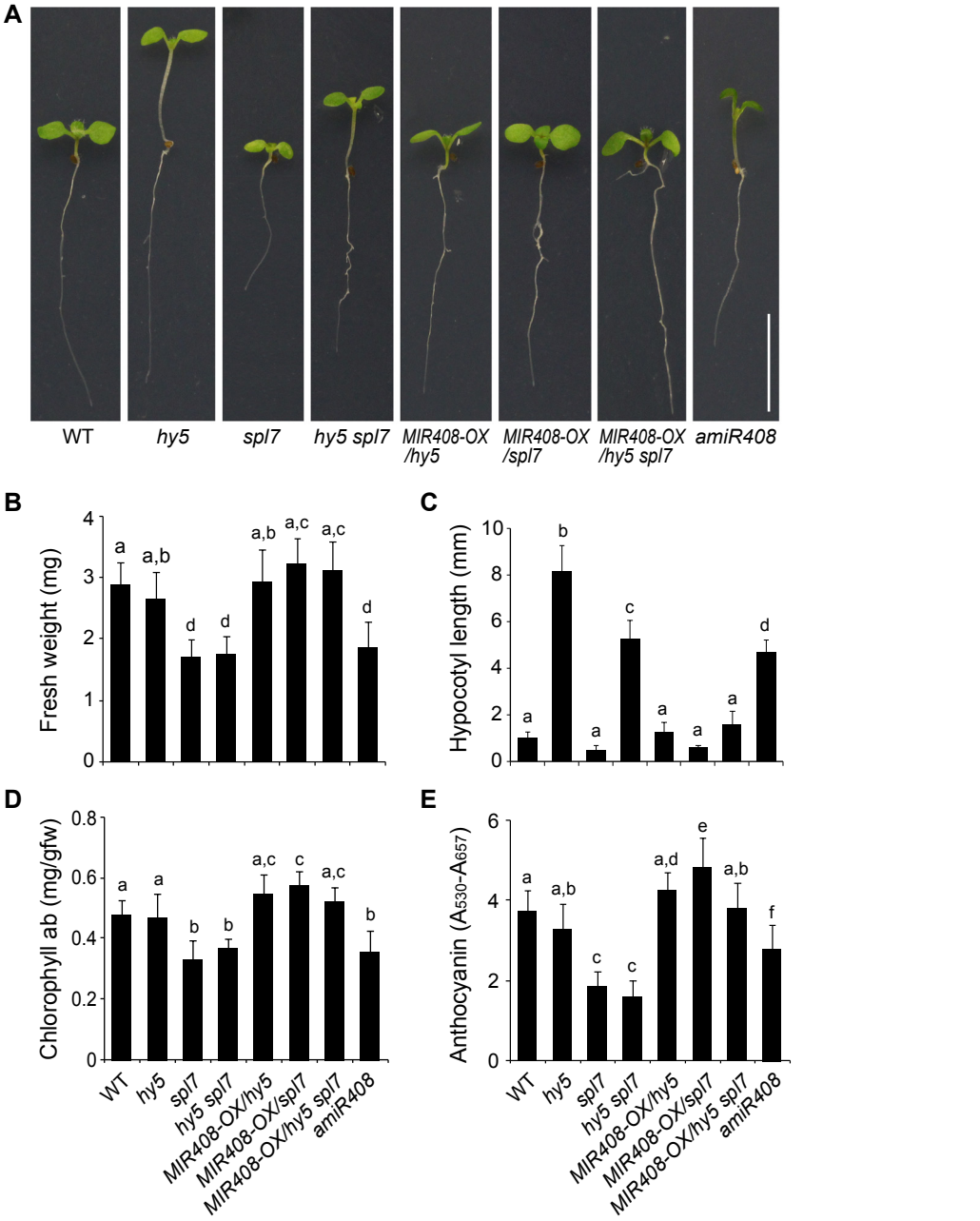

Supplemental Figure 14. Phenotypes of Seedlings Grown with Low Sucrose.
(**A**) Seedling morphology of eight genotypes as indicated in which miR408 accumulates to varied levels. Seedlings were grown under conditions identical to those shown in Figure 7 of the main text except that the MS medium was supplemented with sucrose to a 0.1% (w/v) concentration. Plants were photographed seven days after germination. Bar = 1 cm. (**B**) Quantitative measurement of fresh weight (n = 30), (**C**) hypocotyl length (n = 30), (**D**) chlorophyll (n = 3), and (**E**) anthocyanin (n = 3) in seedlings of the eight genotypes. Data are means ± SD. Genotypes labeled with the same letters have no statistic difference while different letters denote genotypes with significant differences (ANOVA, $p < 0.01$).

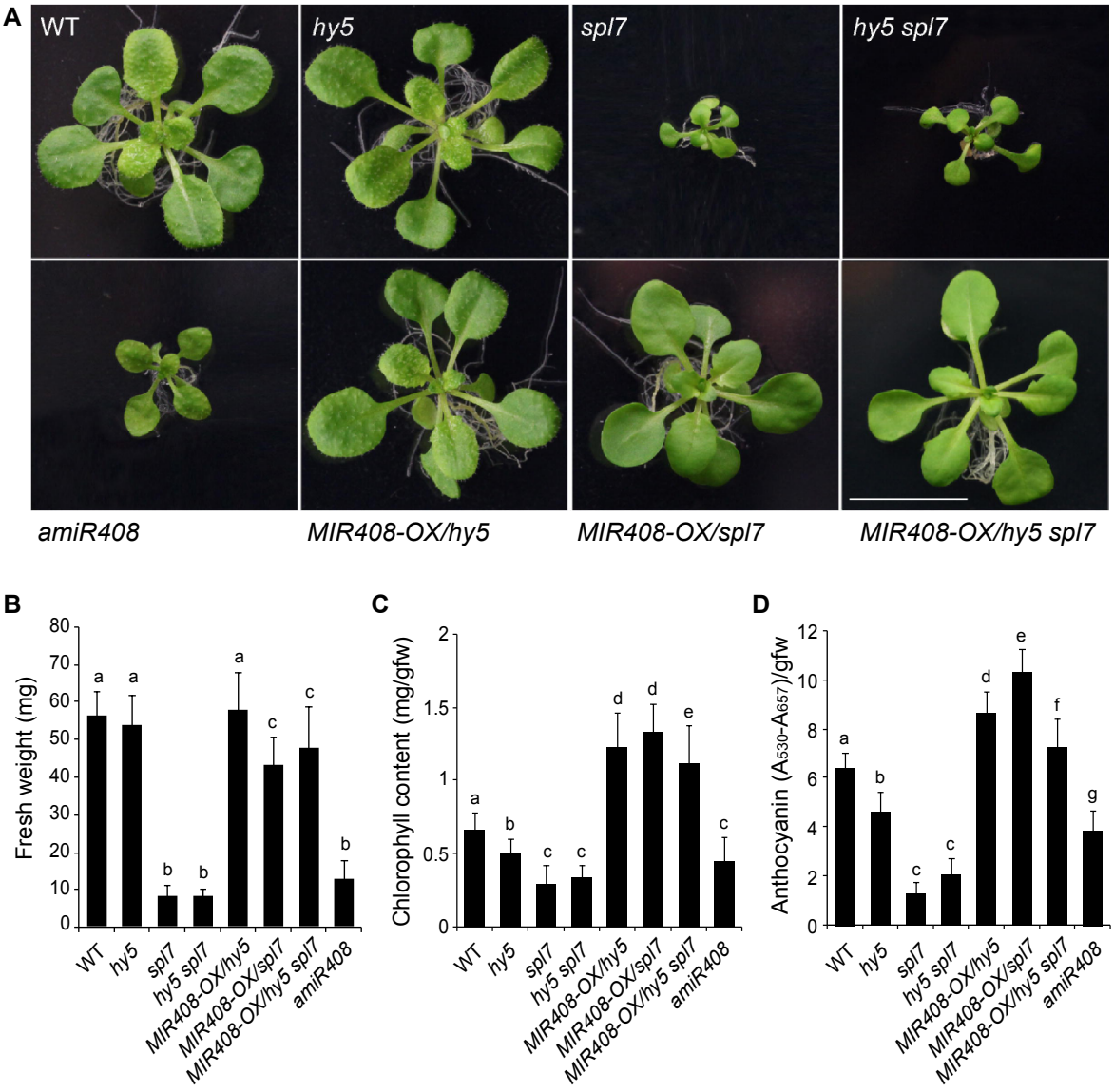

Supplemental Figure 15. Growth Phenotypes of Adult Plants with Altered miR408 Levels.
(**A**) Morphology of adult plants with genotypes as indicated in which miR408 has varied expression levels. Plants were allowed to grow on MS medium containing 1% sucrose under the Light:Dark = 16h:8h condition for three weeks before photographed. Note that the *spl7* mutant contains the *gl1* mutation that inhibits trichome formation and gives the plants glabrous appearance. This recessive mutation was allowed to segregate freely from *spl7* in genetic crosses to create the *hy5 spl7* double mutant. Bar = 1 cm. (**B**) Quantitative measurement of fresh weight (n = 7), (**C**) chlorophyll (n = 3), and (**D**) anthocyanin (n = 3) of adult plants with the indicated genotypes. Data are means ± SD. Genotypes labeled with the same letters have no statistic difference while different letters denote genotypes with significant differences (ANOVA, $p < 0.01$).

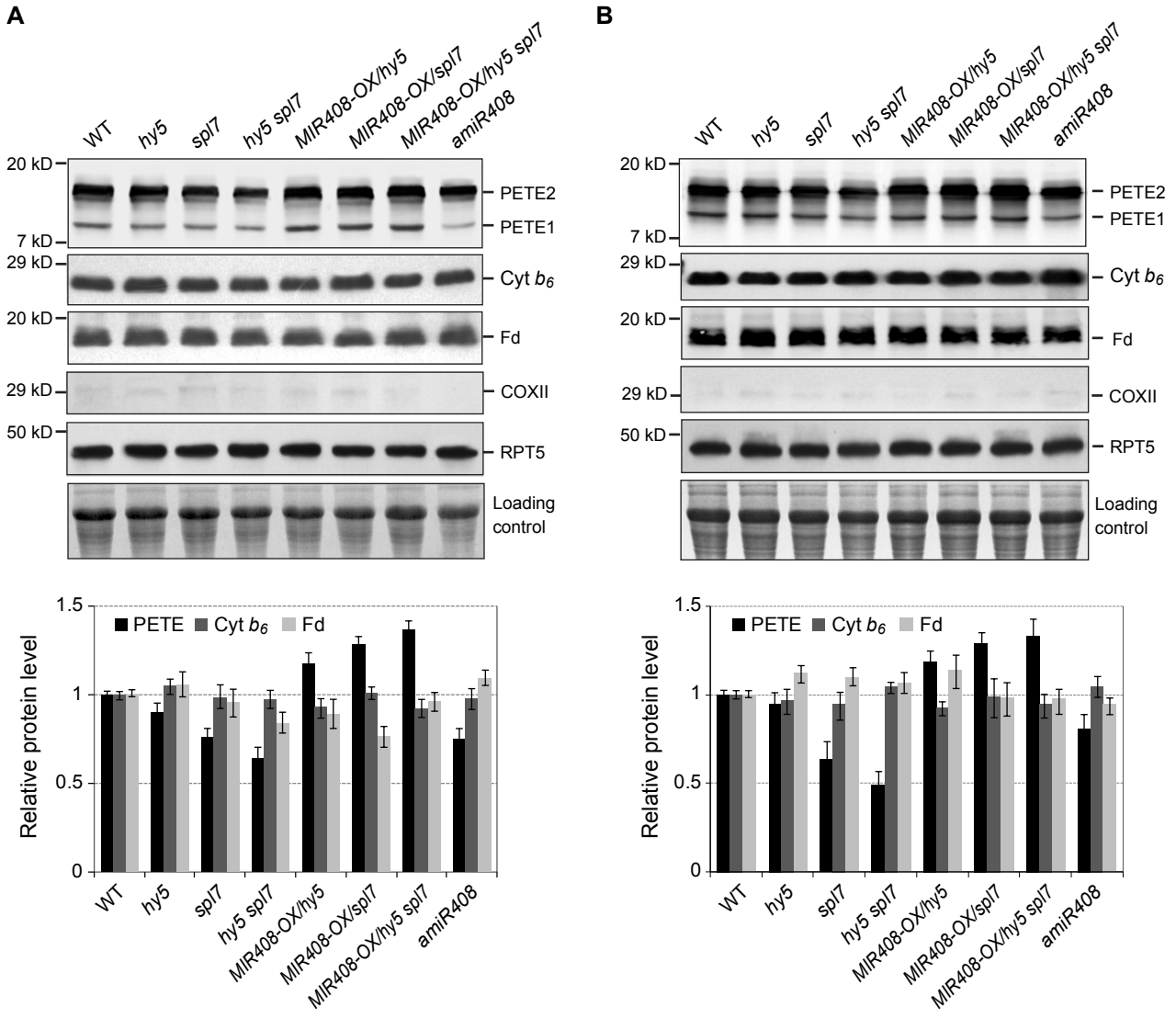

Supplemental Figure 16. Expression of Photosynthetic Electron Carrier Proteins in Seedlings with Varied miR408 Levels. (**A**) Immunoblots (upper panels) and quantification (bottom panel) of photosynthetic electron carrier proteins in plants with altered *MIR408* expression. Plants were grown on MS media supplemented with 1% (w/v) sucrose for seven days. Immunoblotting was performed with antibodies specific to PC (PETE1/2), chloroplast cytochrome b_6 (Cyt b_6), chloroplast ferredoxin (Fd), and mitochondrion cytochrome oxidase subunit II (COXII) proteins in seedlings of indicated genotypes. Relative uniform bands for the chloroplast genome-encoded Fd and mitochondria COXII further support intactness of the assayed chloroplasts. RPT5 was used as the loading control. Blots shown are one representative of three independent experiments. Values represent respective protein levels normalized against RPT5 using Image J and set to one for wild type. (**B**) Same analysis applied to plants grown on MS media supplemented with only 0.1% sucrose.

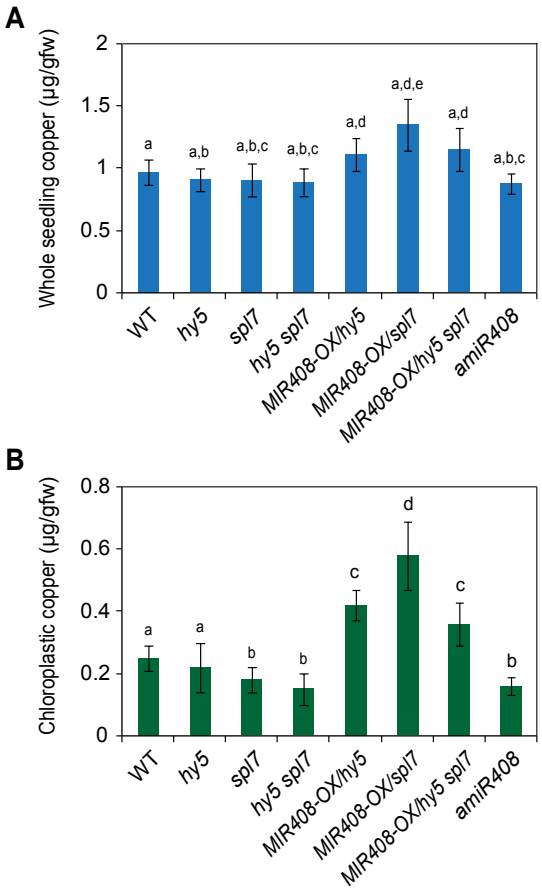

Supplemental Figure 17. Copper Content in Whole Seedlings and the Chloroplast Fractions of Various Genotypes with Altered *MIR408* Expression.

(**A**) Seedlings of the indicated genotypes were grown on MS media supplemented with 1% sucrose under the DC/HL condition for ten days, weighted, desiccated, digested in 1% nitric acid, and used directly for measuring copper content by inductively coupled plasma-atomic emission spectroscopy. (**B**) Intact chloroplasts from seedlings of the indicated genotypes were prepared and measured for copper content as well. Values indicate amounts of copper expressed as $\mu g.g^{-1}$ fresh weight. Data are means ± SD (n = 4). Genotypes labeled with the same letters have no statistic difference while different letters denote genotypes with significant differences (ANOVA, $p < 0.01$).

Supplemental Table 1. Summary of ChIP-seq and RNA-seq data

Sample		Total reads	Unique mapped reads
ChIP-seq	*FLAG-SPL7*	17,790,335	12,280,165 (69%)
	spl7	14,793,925	9,657,327 (62%)
RNA-seq	WT-DC	39,493,611	29,818,770 (75%)
	WT-SC	38,883,416	29,522,234 (76%)
	spl7-DC	43,828,358	33,304,095 (76%)
	spl7-SC	36,451,770	27,467,445 (75%)

FLAG-SPL7, 35S:FLAG-SPL7 transgene; *spl7, spl7* mutant; WT, wild type; DC, Low copper concentration (MS); SC, high copper concentration (MS plus 5μM $CuSO_4$).

Supplemental Table 2. Oligonucleotide sequences for the primers and probes used in this study

Oligo name	Oligo sequence (5' to 3')
For quantitative RT-PCR	
SPL7-F	GAGCTGGAGGGCTATATCCG
SPL7-R	GGAAGAGGCTCGATGACTGT
Plantacyanin-F	GAGGCAGTGCATCATGGTCG
Plantacyanin-R	GAGGTCCGTTTGAATCTTCCA
LAC12-F	TCGGCTTCATTGATTATCGCCAAAG
LAC12-R	TTGTGGTGGCACGCTCACAGCTC
LAC13-F	TTCACTTGTCAATGCAGAAGTTCAC
LAC13-R	TCTCATTATCCGCCCTCCGCTCTC
HY5-F	CCATCAAGCAGCGAGAGGTCATCAA
HY5-R	CGCCGATCCAGATTCTCTACCGGAA
pre-MIR408-F	TGCAATGAAAGAAGACAAAGCG
pre-MIR408-R	GAGAGGTAGACCAAACCCAAAAAC
Atactin7-F	GGTGTCATGGTTGGTATGGGTC
Atactin7-R	CCTCTGTGAGTAGAACTGGGTGC
5SRNA-F	GATGCGATCATACCAGCACTAA
5SRNA-R	GATGCAACACGAGGACTTCCC
For plasmid construction	
AD-SPL7-R	CGGCTCGAGTCAAATTTTGTGTACCAATCTCA
FLAG-SPL7-F	AGTCTAGATGGACTACAAGGACGACGATGACAAATCTTCTCTGTCGCAATCG
FLAG-SPL7-R	TAACTAGTTCAAATTTTGTGTACCAATCTCATTC
p408mut-BF	GGGTCCTACCTCGAGGCAGCTAAATTATTTCT
p408mut-BR	TTAGCTGCCTCGAGGTAGGACCCAAAGTACAT
For EMSA	
Probe G-box-R	GGGTCCTACCACGTGGCAGCTAAA
Probe G-box-F	TTTAGCTGCCACGTGGTAGGACCC
Mutated probe G-box-F	GGGTCCTACCTGCAGGCAGCTAAA
Mutated probe G-box-R	TTTAGCTGCCTGCAGGTAGGACCC
probe VI-F	AAAGTGTACTTGCGATGTACTTTGGGTCCTACCACGTGGCAGC
probe VI-R	GCTGCCACGTGGTAGGACCCAAAGTACATCGCAAGTACACTTT
SPL7-pF	TTAGTAAGCACATGGTGGATG
SPL7-pR	GAGCTATGTAGGAGGAAGTG
MEME-motif-F	TCTTCTTCTCCTTCCTC
MEME-motif-R	GAGGAAGGAGAAGAAGA
For genotyping	
T- spl7-F	TTGGAAATTCAAGCTGATTCG
T- spl7-R	TCCACCTGTCAAAACCAAGAC
LBb1	GCGTGGACCGCTTGCTGCAACT
HY5-GF	GTCATCAAGCTCTGCTCCACAT
HY5-GR	AAGACACCTCTTCAGCCGCTTG
For ChIP-qPCR	
miR408pF	TGCAACCAATACTGAACCAATCCAA
miR408pR	AGTCTTGTACTGCGATCTGGCTAA
SPL7pF	ATAGTAACTTAGTAAGCACATGGTG
SPL7pR	GAGGAGGTGTTGAGCTATGTAG
LAC12pF	TGATTTGTGTATTTGGTAAGACAGGA
LAC12pR	AGAAGTTGAGACATTGAAAGGGAGC
LAC13pF	TGTCTTTGAAGCACTCAAAGTCAC
LAC13pR	CCTACCAGCCTACTTTAGTACCT
At1g58100-FP	ACAGTGGTATGTTCCAATTCTCATC
At1g58100-RP	ATATTATTTTTTAGTTTGTAGTCGGTGC
At1g56380-FP	CATGTTTAGTGATTTTTTCTTCTTGCT
At1g56380-RP	AAATCGATTTTATCTCTTCTTTTCTGTT
At1g27450-FP	CCAAAACATCACCAGCACTTCCT
At1g27450-RP	TGAAAATCCACTCTTGCCTCTCC
At2g45060-FP	GAGCATCGGTTTCATTGCTTTC
At2g45060-RP	AGTCACTTAGGGTGGCATTGTCTT
At3g03780-FP	ACAACACACACCAACTCTCCTCC
At3g03780-RP	GAGAATTATACGTATAACGACGGTTTAC
At4g36040-FP	TGCTTATTATATGGAGGGAGGAGG
At4g36040-RP	ATAGAGATCAAATCTGAAATGACGAGT
At5g03495-FP	TCTTCATTTGTCCTCTGTTTCTCTG
At5g03495-RP	GAGCCTAGTGTCATATCCCTCCA
At5g60740-FP	GCAAATCCTTATCAAAAAGCACTCTC
At5g60740-RP	TTCTTCGTCTCTCCTCTGCCATC
At5g03552-FP	ATGAGCATATTGGGATCTTAAATAGC
At5g03552-RP	TCTAGATACAGTTCGTTTCGTGACAG
At5g46845-FP	CACCATTGTCTTTTTCTATTATGTGCT
At5g46845-RP	TATCTTTATACGTGGATCTTGGCTTG
At2g01120-FP	AGAGACTCCGGCGGAGAAATCC
At2g01120-RP	ATACTGAATCAGGAAACTGCTCC
At5g48840-FP	TACATTAGTTTGCTAGTTAATTC
At5g48840-RP	CCAGAAAACGAGTGAGCCATAAAG
At3g21060-FP	AACCATGAGAGGTTCTCGCAC
At3g21060-RP	GAAGGCGTGAGAACGAAATCG
At4g25100-FP	TACCGGATTGGCTGATCCACT
At4g25100-RP	GAGAAACTCGAACATGAACTAAG
At4g21270-FP	CGTGTAATCCACCCATCGAAG
At4g21270-RP	ACTTCTGGAATTATCATAACG
At5g14565-RP	GGCATCTTTGGAACACTTCCTAG
At5g14565-FP	CACAACAAATGATGAAAGGATTGTG